Channelized Digital Receivers for Impulse Radio

Won Namgoong
Department of Electrical Engineering
University of Southern California
Los Angeles, CA 90089-2562, USA

ABSTRACT

Critical to the design of a digital impulse radio (IR) receiver is the ability of the analog-to-digital converter (ADC) to efficiently sample and digitize the received signal at the signal Nyquist rate of several gigahertz. Since designing a single ADC to operate at such frequencies is not practical, channelized receivers that efficiently sample at a fraction of the signal Nyquist rate are presented. Their performances are compared in the presence of phase noise/sampling jitter and narrowband interference. Our analysis suggests that channelizing the received signal in the frequency domain results in consistently higher performance than channelizing in the time domain. Furthermore, in the presence of moderate sampling jitter/phase noise, high resolution ADC's are not needed.

1. INTRODUCTION

The ultra-wideband (UWB) radio operates by spreading the energy of the radio signal very thinly from near d.c. to a few gigahertz. Since this frequency range is highly populated, the UWB radio must contend with a variety of interfering signals, and it must not interfere with narrowband radio systems operating in dedicated bands. The impulse radio (IR) is an UWB system that uses time-hoping spread spectrum techniques to satisfy these requirements [1][2].

In an IR receiver, the analog-to-digital converter (ADC) can be moved almost up to the antenna as shown in Figure 1. Critical to this design approach, however, is the ability of the ADC to efficiently sample and digitize the received signal at least at the signal Nyquist rate of several gigahertz. The ADC must also support a very large dynamic range to resolve the signal from the strong narrowband interferers. Currently, such ADC's are far from being practical.

As a result, existing UWB receivers perform receiver functions such as correlation in the analog domain before digitizing at a much reduced sampling frequency. Such analog receivers are less flexible and suffer from circuit mismatches and other non-idealities. These circuit non-idealities limit the number of analog correlators that can be practically realized on an integrated circuit (IC). Since over a hundred correlators may be required to exploit the diversity available in an UWB system, existing analog receivers suffer from significant performance loss. The analog circuit non-idealities also preclude the use of sophisticated narrowband interference suppression techniques, which can greatly improve the receiver performance in environments with large narrowband interferers such as in UWB systems. Consequently, to achieve high reception performance, the UWB signal needs to be digitized at the signal Nyquist rate of several gigahertz, so that all of the receiver functions are performed digitally.

Since designing a single ADC to operate at least at the signal Nyquist rate is not practical, parallel ADC architectures with each ADC operating at a fraction of the effective sampling frequency need to be employed. This paper presents two parallel impulse radio digital receivers and compares their performance in the presence of phase nosie/sampling jitter and narrowband interference.

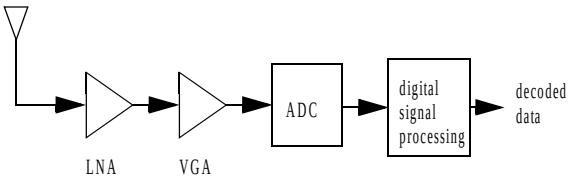

Figure 1 : UWB receiver architecture.

2. RECEIVER ARCHITECTURES

To sample at a fraction of the effective sampling frequency, the received analog signal needs to be channelized either in the time or frequency domain. An approach that has been used in high-speed digital sampling oscilloscopes is to employ an array of M ADC's each triggered successively at $1/M$ the effective sample rate of the parallel ADC. A fundamental problem with an actual implementation of such time-interleaved architecture is that each ADC sees the full bandwidth of the input signal. This causes great difficulty in the design of the sample/hold circuitry. Furthermore, in the presence of strong narrowband interferers, each ADC requires an

This work was supported in part by the Army Research Office under contract number DAAD19-01-1-0477 and National Science Foundation under contract number ECS-0134629.

impractically large dynamic range to resolve the signal from the narrowband interferers.

Instead of channelizing by time-interleaving, the received signal can be channelized into multiple frequency subbands using a bank of bandpass filters and an ADC in each subband channel operating at a fraction of the effective sampling frequency [3]. An important advantage of channelizing the UWB signal in the frequency domain is that the dynamic range requirement of each ADC is relaxed, since the frequency channelization process isolates the effects of a large narrowband interferer. The sample/hold circuitry in the subband ADC, however, is still very difficult to design as it sees the uppermost frequency in the high-frequency subband channels. In addition, sharp bandpass filters with high center frequencies, which are necessary to mitigate the effects of strong narrowband interferers, are extremely difficult to realize especially in integrated circuits.

Instead of using bandpass filters with high center frequencies, channelization can be achieved using a bank of M mixers operating at equally spaced frequencies and M lowpass filters to decompose the analog input signal into M subbands. In addition to obviating the need to design high frequency bandpass filters, channelizing the received signal using this approach greatly relaxes the design requirements of the sample/hold circuitry. The sample/hold circuitry in this architecture sees only the bandwidth of the subband signal; whereas in the bandpass channelization approach, the sample/hold circuitry sees the uppermost frequency in the high-frequency subbands.

3. SYSTEM MODEL

With no loss in generality, we assume a time hopping format with pulse-amplitude modulation (PAM). The transmitted pulse, which is a monocycle on the order of a nanosecond or less in width, is given by

$$x(t) = \sum_i a[\lfloor i/N_f \rfloor]\varphi_{tr}(t - iT_f - c_i T_c) \qquad (1)$$

where

$a[j]$ = jth transmitted symbol.

$\varphi_{tr}(t)$ = normalized Gaussian monocycle.

N_f = number of frames per symbol.

T_f = frame period.

T_c = duration of addressable time delay bin (chip).

c_i = ith time-hopping code; $c_i \in \{0, 1, ..., N_c\text{-}1\}$.

N_c = number of possible hops per frame.

A guard time T_g (= T_f - $N_c T_c$) is introduced to account for procesing delay between successive received frames.

An overall system model is shown in Figure 2. The transmitted pulse is scaled by $\|p\|$, which is the square root of the transmit signal power, then filtered by the transmit antenna, the propagation channel, and the receive antenna, whose impulse responses are denoted as $a_{tr}(t)$, $u(t)$, and $a_r(t)$, respectively. Both $a_{tr}(t)$ and $a_r(t)$ are modeled as differentiators. The resulting signal is corrupted by $n(t)$, which is an additve white Gaussian noise (AWGN) of two-sided noise power spectral density equal to $N_0/2$, and a narrowband interferer $I(t)$. The corrupted signal is then passed through an anti-alias filter, $\varphi_{alias}(t)$, which is assumed to be an ideal lowpass filter with a gain transfer of $\sqrt{1/f_{eff}}$ over the frequency range of $-\pi f_{eff} \le \Omega \le \pi f_{eff}$, where f_{eff} is the effective sampling frequency. For comparison purposes, the resulting signal, $s(t)$, is the input to both a time channelized and frequency channelized receivers. Signal $s(t)$ can be written as

$$s(t) = \sum_i a[\lfloor i/N_f \rfloor]\varphi_p(t - iT_f - c_i T_c) + n_p(t) \qquad (2)$$

where $\varphi_p(t) = \|p\|\varphi''_{tr}(t) \otimes \varphi_{alias}(t) \otimes u(t)$, $\varphi''_{tr}(t)$ is the second derivative of $\varphi_{tr}(t)$, and $n_p(t) = (n(t) + I(t)) \otimes \varphi_{alias}(t)$. Although the anti-alias filter is not needed in the frequency channelized receiver, it is employed so that a fair comparison can be made between the two receivers.

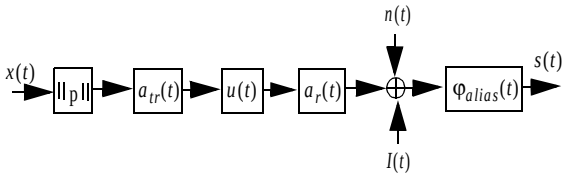

Figure 2 : Overall system model.

In an impulse radio, sampling does not need to be performed continuously since the signal is transmitted in bursts. For example, sampling in the ith frame begins at a time Δ before the arrival of the ith pulse and continues until N_s samples are collected. The first sampling time in the ith frame is denoted as γ_i, where

$$\gamma_i = iT_f + c_i T_c - \Delta \qquad (3)$$

Although the pulse in one frame may overlap with the next because of multipaths, we assume for ease of explanation that T_g is sufficiently large that successive pulses never overlap.

3.1 Time-interleaved receiver

A time-interleaved receiver with M channels is shown in Figure 3. In the kth channel, the lth sample for the ith frame after quantization is

$$s^{(t)}_{k,i}[l] = a[\lfloor i/N_f \rfloor]x^{(t)}_{k,i}[l] + n^{(t)}_{k,i}[l] \qquad (4)$$

where

$$x^{(t)}_{k,i}[l] = \varphi_p(-\Delta + (lM + k)/f_{eff} + \tau_k[l]) \qquad (5)$$

$$n_{k,i}^{(t)}[l] = n_p(-\Delta + (lM + k)/f_{eff} + \tau_k[l]) + n_{q_k}^{(t)}[l] \quad (6)$$

In (4)-(6), the superscript (t) denotes the time-interleaved receiver, and $\tau_k[l]$ and $n_{q_k}^{(t)}[l]$ are the sample-time offset and the quantization noise on the lth sample in the kth channel. The sampled and digitized signal $s_{k,i}^{(t)}[l]$ is correlated with the template sequence $\{w_k^{(t)}[l]\}$ then summed as shown in Figure 3. The template sequence $\{w_k^{(t)}[l]\}$ is repeated at every frame for the entire symbol period and updated after every symbol period.

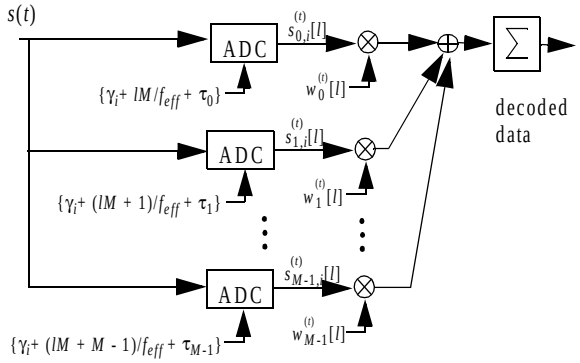

Figure 3 : Time-channelized receiver with M channels.

3.2 Frequency channelized receiver

A frequency channelized receiver is shown in Figure 4. It employs a bank of complex mixers operating at equally spaced frequencies (denoted as f_1, f_2, ..., f_{M-1}) and lowpass filters (denoted as H(jΩ)) to decompose the analog input signal into M subbands. The lowpass filter H(jΩ) should be designed to have sharp rolloffs with large attenuation in the stopband frequency, since it results in greater robustness to strong narrowband interferers as described in subsequent sections. The M-1 mixer phases, which are time-varying due to the oscillator phase noise, are denoted as $\theta_1(t)$, $\theta_2(t)$, ..., $\theta_{M-1}(t)$. The mixer frequencies are chosen to be multiples of each other (i.e., $f_a = af_1$, $a \in \{1, 2, \ldots, M-1\}$), because a simple frequency divider can then be used to generate the multiple frequencies. To minimize the ADC sampling frequency, the ADC sampling frequency f_{adc} is chosen to be f_1 and the cutoff frequency of H(jΩ) to be $f_{adc}/2$. This frequency choice, which correspond to a maximally decimated filter bank, achieves an effective sampling frequency of $(2M\text{-}1)f_{adc}$.

The sampled signals are then correlated with a template sequence. The results in the non-zero subband channels are converted to a real signal before summing as shown in Figure 4. The real operator is necessary since the transmitted signal is a real signal.

The sampled signal becomes time-invariant when $f_{adc} = f_1$ despite the presence of the mixer. Hence, after some straightforward manipulations, the lth sample in the kth channel and the ith frame after quantization becomes

$$s_{k,i}^{(f)}[l] = a[\lfloor i/N_f \rfloor]x_{k,i}^{(f)}[l] + n_{k,i}^{(f)}[l] \quad (7)$$

where

$$x_{k,i}^{(f)}[l] = e^{-j\Omega_k t}(h_k(t) \otimes \varphi_p(t - iT_f - c_iT_c)e^{j\theta_k(t)})\Big|_{t = \gamma_i + \tau_k[l] + l/f_{adc}} \quad (8)$$

$$n_{k,i}^{(f)}[l] = e^{-j\Omega_k t}(h_k(t) \otimes n_p(t)e^{j\theta_k(t)})\Big|_{t = \gamma_i + \tau_k[l] + l/f_{adc}} + n_{q_k}^{(f)}[l] \quad (9)$$

where superscript (f) denotes the frequency channelized receiver, $\Omega_k = 2\pi f_k$ with $f_0 = 0$, and $h_k(t) = h(t)e^{j\Omega_k t}$.

4. PERFORMANCE ANALYSIS

4.1 Time channelizer analysis

The sampling times of a time-interleaved receiver are generally not equally spaced in time due to circuit non-idealities. The difference from the ideal sampling times are modeled with a static and a zero mean dynamic sample-time offsets. The slow drifts that are present in an actual sampler are assumed to be small over the time interval of interest. Thus, the lth sample-time offset in the kth channel can be written as $\tau_k[l] = \tau_{k,0} + \Delta\tau_k[l]$, where $\tau_{k,0}$ and $\Delta\tau_k[l]$ represent the static and dynamic sample-time offsets, respectively.

Assuming $\Delta\tau_k[l] \ll 1/f_{adc}$ and linearizing about the nominal sampling time, the lth sample in the ith frame and the kth channel after quantization is

$$s_{k,i}^{(t)}[l] = a\bar{x}_{k,i}^{(t)}[l] + \bar{n}_{k,i}^{(t)}[l] + a\tilde{x}_{k,i}^{(t)}[l] + \tilde{n}_{k,i}^{(t)}[l] \quad (10)$$

where a is the transmitted symbol with the time index omitted for notational brevity, $\bar{x}_{k,i}^{(t)}[l]$ and $\bar{n}_{k,i}^{(t)}[l]$ are given in (5) and (6) with $\tau_k[l]$ replaced with $\tau_{k,0}$, and

$$\tilde{x}_{k,i}^{(t)}[l] = \varphi_p'(-\Delta + (lM + k)/f_{eff} + \tau_{k,0}) \cdot \Delta\tau_k[l] \quad (11)$$

$$\tilde{n}_{k,i}^{(t)}[l] = n_p'(-\Delta + (lM + k)/f_{eff} + \tau_{k,0}) \cdot \Delta\tau_k[l] \quad (12)$$

In (11) and (12), $\varphi_p'(.)$ and $n_p'(.)$ denote the derivatives of $\varphi_p(.)$ and $n_p(.)$, respectively.

The dynamic sample-time offset $\Delta\tau_k[l]$ is assumed to be approximately uncorrelated from sample-to-sample and from channel-to-channel, i.e.,

$$E\{\Delta\tau_k[l + u]\Delta\tau_m[l]\} \approx \delta[k - m]\delta[u]\sigma_{\Delta\tau}^2 \quad (13)$$

where $\sigma_{\Delta\tau}^2$ is the jitter or the variance of $\Delta\tau_k[.]$.

All the samples in the ith frame given in (10) can be represented using vectors as

$$\boldsymbol{Y}_i = a\boldsymbol{X}_i + \boldsymbol{N}_i + a\tilde{\boldsymbol{X}}_i + \tilde{\boldsymbol{N}}_i \quad (14)$$

where $\boldsymbol{X}_i = [\bar{x}_{0,i}^{(t)}[0] \;\; \bar{x}_{1,i}^{(t)}[0] \;\; \ldots \;\; \bar{x}_{M-1,i}^{(t)}[N_s-1]]^T$. $\boldsymbol{N}_i$, $\tilde{\boldsymbol{X}}_i$, and $\tilde{\boldsymbol{N}}_i$ are vectors with elements $\bar{n}_{k,i}^{(t)}[l]$, $\tilde{x}_{k,i}^{(t)}[l]$, and $\tilde{n}_{k,i}^{(t)}[l]$, respectively, that are indexed as in $\boldsymbol{X}_i$. The template sequence is also represented as a vector $\boldsymbol{W} = [w_0^{(t)}[0] \;\; \ldots \;\; w_{M-1}^{(t)}[N_s-1]]^T$. For the zeroth transmitted symbol, the decoded symbol $\hat{a}[0]$ is given by

$$\hat{a}[0] = \sum_{i=0}^{N_f-1} \boldsymbol{W}^T \boldsymbol{Y}_i \quad (15)$$

The template sequence that estimates the transmitted signal in the minimum mean squared error (MMSE) sense is

$$\boldsymbol{W}_{mmse} = \boldsymbol{R}_{a\boldsymbol{Y}} \boldsymbol{R}_{\boldsymbol{YY}}^{-1} \quad (16)$$

where $\boldsymbol{R}_{a\boldsymbol{Y}} = E\{a\boldsymbol{Y}_i^H\}$ and $\boldsymbol{R}_{\boldsymbol{YY}} = E\{\boldsymbol{Y}_i \boldsymbol{Y}_i^H\}$. The corresponding unbiased SNR of the decoded symbol is

$$SNR = N_f \cdot \frac{\boldsymbol{W}_{mmse} \boldsymbol{R}_{a\boldsymbol{Y}}^H}{1 - \boldsymbol{W}_{mmse} \boldsymbol{R}_{a\boldsymbol{Y}}^H} \quad (17)$$

4.2 Frequency channelizer analysis

4.2.1 Phase noise model

In addition to the sample-time offsets, the frequency-channelized receiver suffers from the effects of the mixer phase noise. In the time interval range of interest, the phase of the kth subband mixer, $\theta_k(t)$, is assumed to consist of a static phase offset $\theta_{k,0}$ and a zero mean random phase noise $\Delta\theta_k(t)$, i.e., $\theta_k(t) = \theta_{k,0} + \Delta\theta_k(t)$. Since directly analyzing the effects of the mixer phase noise is difficult, it is approximated by a second order Taylor series expansion about the static phase offset [4], i.e.,

$$e^{j\theta_k(t)} \approx e^{j\theta_{k,0}} \left(1 + j\Delta\theta_k(t) - \frac{\Delta\theta_k^2(t)}{2}\right) \quad (18)$$

The approximation in (18) holds when $\Delta\theta_k(t) \ll 1$, which is a valid approximation. $\Delta\theta_k(t)$ is assumed to be a wide-sense stationary random process with a correlation function given by

$$E\{\Delta\theta_k(t+\tau)\Delta\theta_m(t)\} = \delta[k-m]\sigma_{\Delta\theta}^2 e^{-2\pi f_{3\text{dB}}|\tau|} \quad (19)$$

where $\sigma_{\Delta\theta}^2$ is the variance of the phase noise and $f_{3\text{dB}}$ is the 3-dB bandwidth of the phase noise spectrum. Since the mixer and the sampler are based on the same clock, $\sigma_{\Delta\theta}^2$ is related to the sampling jitter by

$$\sigma_{\Delta\theta}^2 = (2\pi f_{adc})^2 \sigma_{\Delta\tau}^2 \quad (20)$$

4.2.2 MMSE template sequence

Linearizing about the nominal sampling time, the lth sample in the ith frame and the kth channel after quantization is

$$s_{k,i}^{(f)}[l] = a\bar{x}_{k,i}^{(f)}[l] + \bar{n}_{k,i}^{(f)}[l] + a\tilde{x}_{k,i}^{(f)}[l] + \tilde{n}_{k,i}^{(f)}[l] \quad (21)$$

where $\bar{x}_{k,i}^{(f)}[l]$ and $\bar{n}_{k,i}^{(f)}[l]$ are given in (8) and (9) with $\tau_k[l]$ replaced by $\tau_{k,0}$, and

$$\tilde{x}_{k,i}^{(f)}[l] = e^{-j\Omega_k t}(\varphi_p(t - iT_f - c_i T_c) e^{j\theta_k(t)} \otimes (-j\Omega_k h_k(t) + h_k'(t)))\Big|_{t=\gamma_i+\tau_{k,0}+l/f_{adc}} \cdot \Delta\tau_k[l] \quad (22)$$

$$\tilde{n}_{k,i}^{(f)}[l] = e^{-j\Omega_k t}(n_p(t) e^{j\theta_k(t)} \otimes (-j\Omega_k h_k(t) + h_k'(t)))\Big|_{t=\gamma_i+\tau_{k,0}+l/f_{adc}} \cdot \Delta\tau_k[l] \quad (23)$$

The MMSE template sequence and the corresponding SNR are obtained using (16) and (17) with the correlation functions based on the samples in (21). By replacing occurances of $e^{j\theta_k(t)}$ in $\bar{x}_{k,i}^{(f)}[l]$, $\bar{n}_{k,i}^{(f)}[l]$, $\tilde{x}_{k,i}^{(f)}[l]$, and $\tilde{n}_{k,i}^{(f)}[l]$ with the phase noise approximation given in (18), the correlation functions needed to compute the MMSE template sequence and the corresponding unbiased SNR are readily determined.

5. RESULTS AND DISCUSSION

The unbiased SNR of the decoded symbol in the time-interleaved and frequency-channelized receivers are compared. Throughout this section, we assume that both receivers employ the same number of ADC's with each operating at the same frequency. The effective sampling frequency f_{eff} are set to be $2/\sigma$, where σ is the standard deviation of the Gaussian transmit pulse. The ADC frequency f_{adc} is set to $f_{eff}/9$. These frequency choices correspond to $M = 9$ and $M = 5$ for the time-interleaved and frequency-channelized receivers, respectivley. We assume that $f_{3\text{dB}} = 0.01 f_{adc}$ and for simplicity the propagation channel $u(t)$ is an ideal delta function.

Figure 5 plots the unbiased SNR of a single received monocycle at the output of the time-interleaved and frequency-channelized receivers against the standard deviation of the normalized sampling jitter $\sigma_{\Delta\tau} \cdot f_{adc}$. No narrowband interferer is assumed present. There are two plots drawn for each receiver with the top and bottom curves corresponding to when 12-bit and 4-bit ADC's are employed, respectively. The frequency channelized receiver outperforms the time-interleaved receiver with the difference increasing with jitter. This is because the reduced signal bandwidth to each sampler in the frequency-channelized receiver

reduces the amount of aliasing caused by sampling jitter.

The assumptions in Figure 6 are identical to Figure 5 except for the presence of a narrowband interferer, which is assumed to be a real brickwall narrowband interferer with center frequency of $0.25/\sigma$, magnitude of 50dB greater than $N_0/2$, and bandwidth of $0.1/\sigma$. When 4-bit ADC's are employed, the frequency channelized receiver outperforms the time-interleaved receiver by approximately 10dB regardless of the amount of jitter present. When 12-bit ADC's are employed, the performance difference between the two receivers is small for low jitter but increases with increasing jitter. Their performance eventually converges to that of when 4-bit ADC's are employed as shown in Figure 6. This convergence suggests that increasing the ADC resolution to suppress the effects of the narrowband interferer diminishes with increasing jitter and that the use of low resolution ADC's is adequate.

6. CONCLUSION

Two practical digital receivers for impulse radio are presented and their performance analyzed by computing the unbiased SNR when a MMSE template sequence is employed. Our analysis indicate that the frequency-channelized receiver consistently outperforms the time-channelized receiver. In addition, when moderate sampling jitter and mixer phase noise are present, low resolution (e.g. 4-bit) ADC's are sufficient for effectively suppressing the effects of the narrowband interferer.

REFERENCES

[1] M. Win, R. Scholtz, "Impulse Radio: How it Works," IEEE Comm. Letters, vol. 2, no. 10, Jan. 1998.

[2] M. Win, R. Scholtz, "Ultra-Wide Bandwidth Time-Hopping Spread-Spectrum Impulse Radio for Wireless Multiple-Access Communications," IEEE Trans. Commun., vol. 48, no. 4, pp. 679-692, Apr. 2000.

[3] A. Petraglia, et. al., "High Speed A/D Conversion Using QMF Banks," Proc. IEEE Int. Symp. Circuits Syst., pp. 2797-2800, 1990.

[4] P. Robertson, S. Kaiser, "Analysis of the Effects of Phase Noise in Orthogonal Frequency Division Multiple (OFDM) Systems," IEEE. Intern. Conf. on Comm., pp. 1652-1657, 1995.

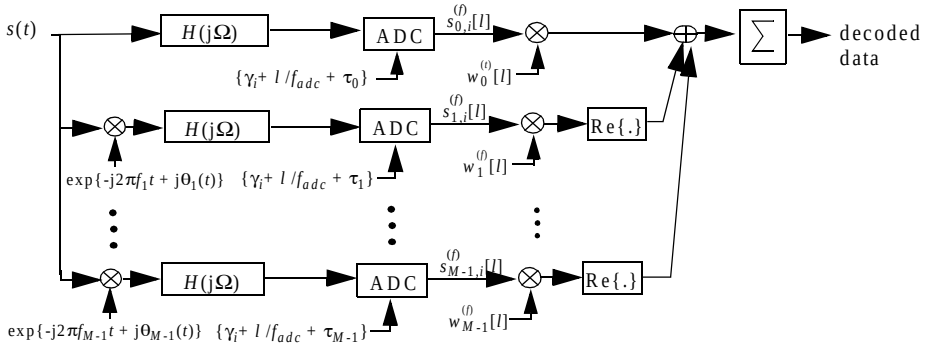

Figure 4 : Frequency-channelized receiver with M subband channels.

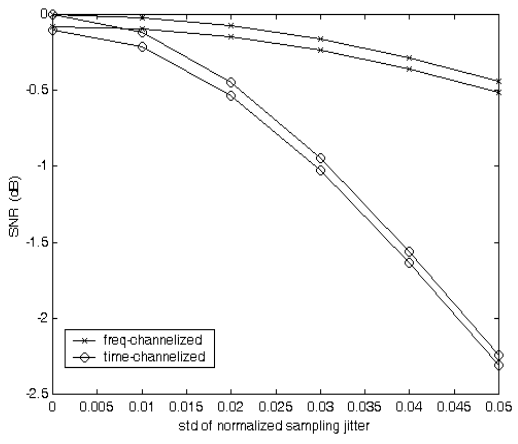

Figure 5 : Effect of sampling jitter/phase noise with no narrowband interference.

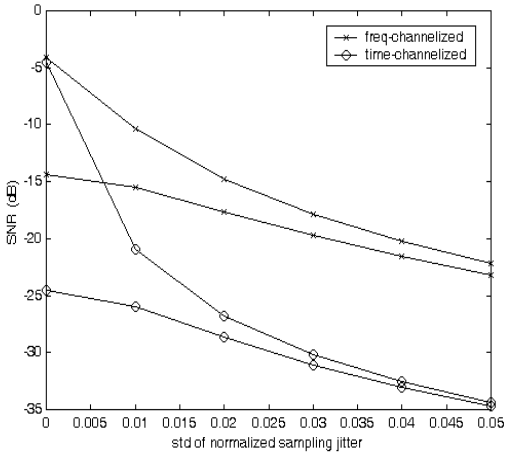

Figure 6 : Effect of sampling jitter/phase noise with narrowband interferer present.